Facile Synthesis, Crystal Structures, and High-Spin Cationic States of All-*para*-Brominated Oligo(*N*-phenyl-*m*-aniline)s

Akihiro Ito,[†] Haruhiro Ino,[†] Kazuyoshi Tanaka,*[,†] Katsuichi Kanemoto,[‡] and Tatsuhisa Kato*[,‡]

Department of Molecular Engineering, Graduate School of Engineering, Kyoto University, Sakyo-ku, Kyoto 606-8501, Japan, and Institute for Molecular Science, Myodaiji, Okazaki 444-8585, Japan

a51053@sakura.kudpc.kyoto-u.ac.jp

Received August 25, 2001

Syntheses of both the dimer (**3**) and the trimer (**4**) of all-*para*-brominated poly(*N*-phenyl-*m*-aniline)s (**2c**) were achieved in a one-pot procedure from the parent nonbrominated oligomers and benzyltrimethylammonium tribromide [(BTMA)Br_3]. An X-ray crystallographic analysis revealed that **4** has a U-shaped structure, suggesting that **2c** easily adopts helical structures. Furthermore, the redox properties were investigated by the UV−vis and EPR measurements. It was confirmed that the both **3** and **4** can be oxidized into the dications $\mathbf{3}^{2+}$ and $\mathbf{4}^{2+}$ with triplet spin-multiplicity.

Introduction

It is well-known that triarylamines often give stable cation radicals.[1] In particular, tris(*p*-bromophenyl)-aminium hexachloroantimonate ($\mathbf{1}^+$),[2] generated by one-electron oxidation of tris(*p*-bromophenyl)amine (TBPA, **1**) using $SbCl_5$, is one of the famous thermally stable radicals and has long been used as a powerful one-electron oxidant in organic synthetic chemistry.[3]

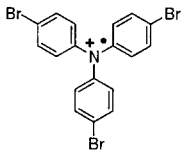

$\mathbf{1}^+$

In view of their stability, triarylamine cation radicals have also become promising spin-containing molecular units for exploitation of potential polymer-based organic magnets. If such triarylamine cation radicals are connected to each other via *meta*-linkage as shown below, the resulting poly(cation radical) of poly(*N*-phenyl-*m*-aniline) (**2a**) is anticipated to have high-spin correlation, leading to a polymer-based magnet.[4] Therefore, chemical and physical properties of oligo(*N*-phenyl-*m*-aniline)s and their polycationic species are of interest from the viewpoint of exploitation of organic high-spin polymers.

Recently, Hartwig and co-workers have succeeded in preparation of several oligomers up to hexadecamer of poly(*N*-anisyl-*m*-aniline)s (**2b**) and, furthermore, the magnetic properties of their oxidized species have been

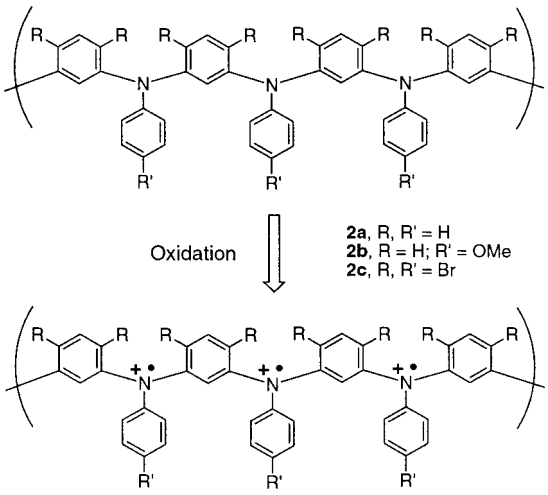

investigated in detail.[5] However, the structural features have not been clarified in their studies. On the other hand, despite the stability of $\mathbf{1}^+$, all-*para*-brominated oligo(*N*-phenyl-*m*-aniline)s have not been hitherto prepared to the best of our knowledge. In this paper, we report on the synthesis, structures, and high-spin cationic states of the dimer (**3**) and the trimer (**4**) of **2c**, which are expected to be thermally stable bis- and tris-cation radicals.

Results and Discussion

Synthesis. Synthesis of **3** and **4** was carried out by the procedure shown in Scheme 1. The completely unsubstituted dimer and trimer, **5** and **6**, were first prepared using the Ullmann reaction from corresponding arylamines and aryl halides. The selective bromination at all *para*-positions succeeded by use of benzyltrimethylammonium tribromide [(BTMA)Br_3].[6] Other powerful brominating agents such as Br_2 and tetrabutylammo-

[†] Kyoto University.
[‡] Institute for Molecular Science.

(1) Forrester, A. R.; Hay, J. M.; Thomson, R. H. *Organic Chemistry of Stable Free Radicals*; Academic Press: New York, 1968.
(2) Bell, F. A.; Ledwith, A.; Sherrington, D. C. *J. Chem. Soc.* **1969**, 2720.
(3) Dapperheld, S.; Steckhan, E.; Brinkhaus, K. G.; Esch, T. *Chem. Ber.* **1991**, *124*, 2557−2567 and references therein.
(4) (a) Ito, A.; Ota, K.; Tanaka, K.; Yamabe, T.; Yoshizawa, K. *Macromolecules* **1995**, *28*, 5618. (b) Yoshizawa, K.; Takata, A.; Tanaka, K.; Yamabe, T. *Polym. J.* **1992**, *24*, 857.
(5) (a) Louie, J.; Hartwig, J. F. *Macromolecules* **1998**, *31*, 6737. (b) Goodson, F. E.; Hauck, S. I.; Hartwig, J. F. *J. Am. Chem. Soc.* **1999**, *121*, 7527.

10.1021/jo0160571 CCC: $22.00
Published on Web 01/03/2002

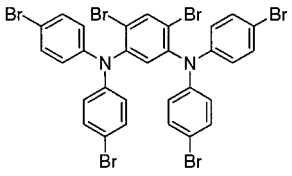

3

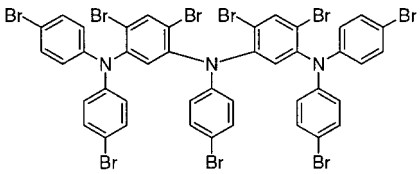

4

nium tribromide [(TBA)Br_3][7] were met with failure. The brominated products **3** and **4** were isolated as single crystals suitable for X-ray analysis by slow evaporation of the solvent from the reaction mixture. The recrystallization of **5** from CH_2Cl_2 gave colorless needles suitable for X-ray crystallographic study. Single crystal of **6** was unavailable despite our several attempts.

Molecular Structures of 3−5. The crystal of **5** contains two crystallographically independent but conformationally same molecules owing to its space group (C_c). The molecular structure of **5** (Figure 1) is very similar to that of *N*,*N*,*N*′,*N*′,*N*″,*N*″-hexaphenyl-1,3,5-triaminobenzene.[8] As has been investigated by Veciana and co-workers, triphenylmethyl-based molecules have the combined helicity due to their propeller-like structure.[9] The same structural characterization is applicable to the present triphenylamine-based molecules. In **5**, the molecule adopts an approximate C_s conformation (in other words, a *meso* (*P**,*M**) form). On the other hand, the crystal of **3** contains dichloromethane, one of the components of the mixed solvents, in ratio of 1:1 with **3**, as shown in Figure 2. Interestingly, **3** is approximately C_2-symmetric (in other words, either (*P*,*P*) or (*M*,*M*) form), while the degree of off-coplanarity in each phenyl group remains unchanged regardless of existence of bromo substituents. Figure 3 shows two kinds of views of the molecular structure of **4**. The conformation of **4** is of either (*M*,*P*,*P*) or (*P*,*M*,*M*) form. As is evident from Figure 3b, **4** favors a U-shape conformation. This closely relates to the fact that a nonnegligible quantity of cyclic oligomers were obtained in the preparation of poly(*N*-aryl-*m*-aniline) by Hartwig's group.[5]

Electrochemical Studies. Redox behaviors of these oligomers were studied by cyclic voltammetry (CV) at room temperature. The electrochemical data for **3**−**6** and their related triarylamines are summarized in Table 1.

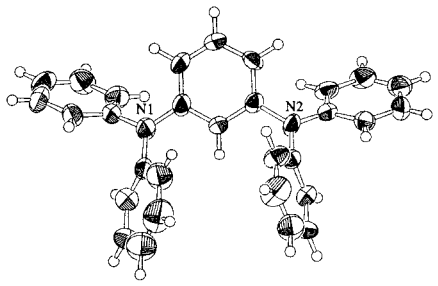

Figure 1. Molecular structure of **5**.

Scheme 1. Preparation of Compounds 3 and 4

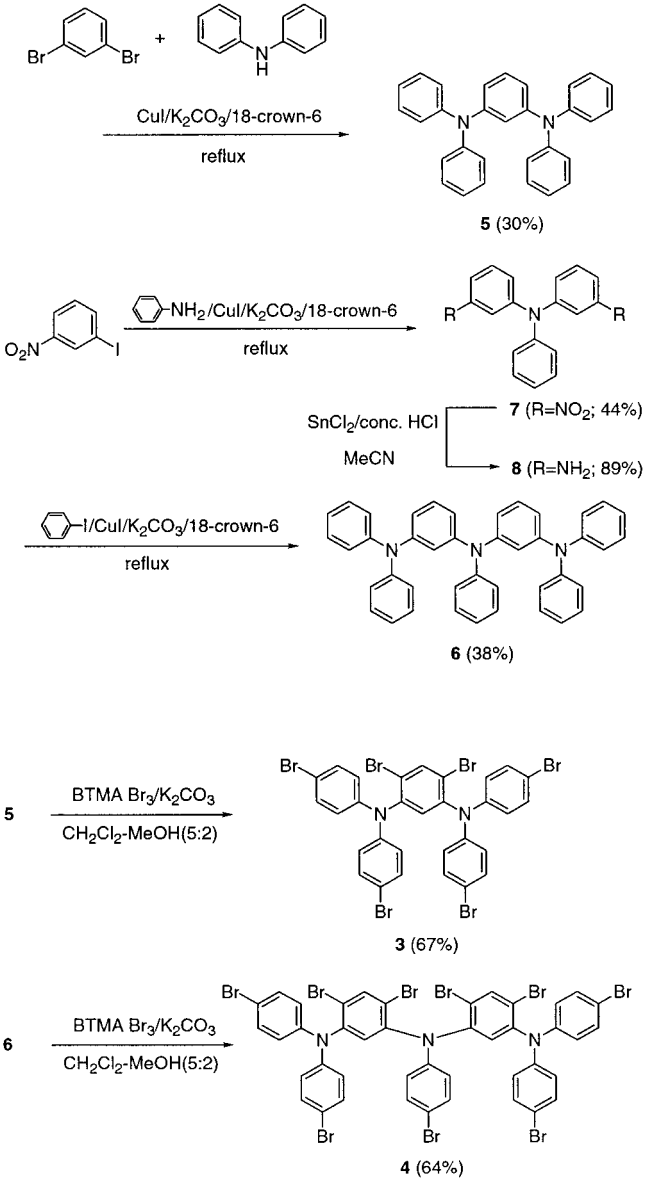

First of all, both **5** and **6** exhibited only one irreversible oxidation wave. In the reverse scan, some new peaks appeared in both **5** and **6**, indicating the reduction process of the redox-active products generated by the follow-up reactions. Moreover, in **6**, a new oxidation peak was observed at the lower potential (+0.66 V vs SCE) in the second sweep. In a cyclic voltammetric study of a series of 1,3-bis(diarylamino)benzenes, the protecting substituents on the both central and peripheral phenyl rings are found to be important to stabilize the dicationic

(6) Kajigaeshi, S.; Kakinami, T.; Inoue, K.; Kondo, M.; Nakamura, H.; Fujikawa, M.; Okamoto, T. *Bull. Chem. Soc. Jpn.* **1988**, *61*, 597.

(7) (a) Berthelot, J.; Guette, C.; Essayegh, M.; Desbene, P. L.; Basselier, J. J. *Synth. Commun.* **1986**, *16*, 1641. (b) Berthelot, J.; Guette, C.; Essayegh, M.; Desbene, P. L.; Basselier, J. J. *Can. J. Chem.* **1989**, *67*, 2061.

(8) Yoshizawa, K.; Chano, A.; Ito, A.; Tanaka, K.; Yamabe, T.; Fujita, H.; Yamauchi, J.; Shiro, M. *J. Am. Chem. Soc.* **1992**, *114*, 5994.

(9) (a) Veciana, J.; Rovira, C.; Crespo, M. I.; Armet, O.; Domingo, V. M.; Palacio, F. *J. Am. Chem. Soc.* **1991**, *113*, 2552. (b) Veciana, J.; Rovira, C.; Ventosa, N.; Crespo, M. I.; Palacio, F. *J. Am. Chem. Soc.* **1993**, *115*, 57. (c) Sedó, J.; Ventosa, N.; Ruiz-Molina, D.; Mas, M.; Molins, E.; Rovira, C.; Veciana, J. *Angew. Chem., Int. Ed. Engl.* **1998**, *37*, 330. (d) Ventosa, N.; Ruiz-Molina, D.; Sedó, J.; Rovira, C.; Tomas, X.; André, J.-J.; Bieber, A.; Veciana, J. *Chem. Eur. J.* **1999**, *5*, 3533.

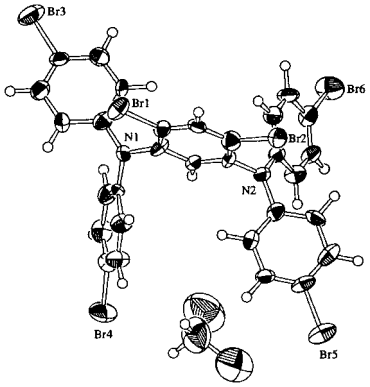

Figure 2. Molecular structure of **3**.

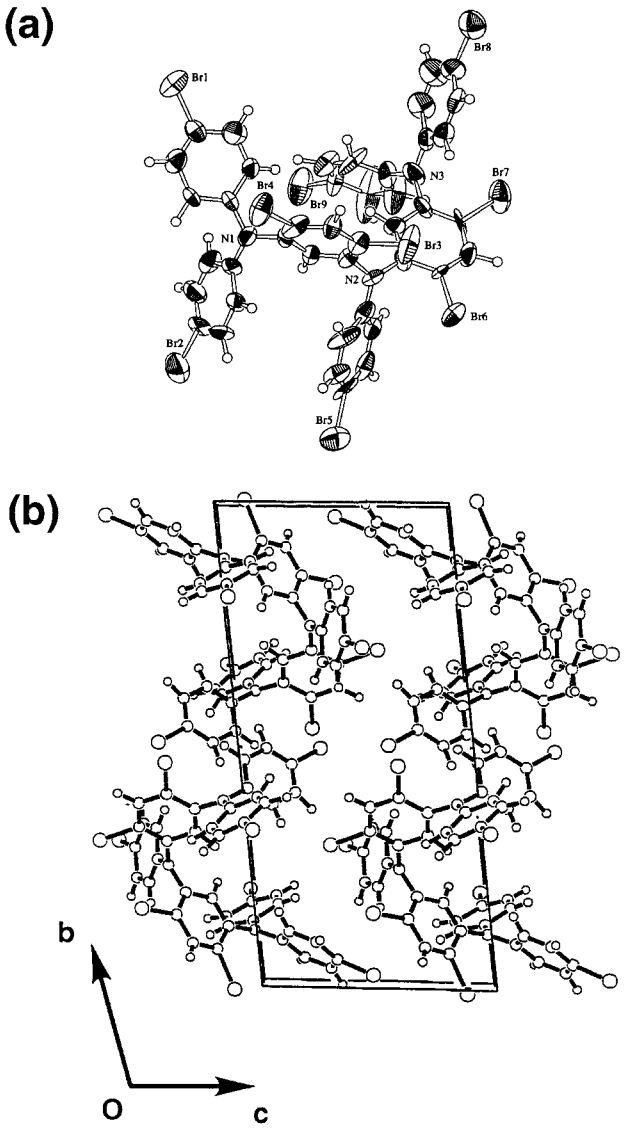

Figure 3. (a) Molecular structure and (b) packing diagram of **4**.

species.[10] In this respect, the redox irreversibility of **5** and **6** was expected to some extent. On the other hand, it was found that the Br-substituted oligomers **3** and **4** satisfy the criterion of the redox reversibility. As shown

(10) Yano, M.; Sato, K.; Shiomi, D.; Ichimura, A.; Abe, K.; Takui, T.; Itoh, K. *Tetrahedron Lett.* **1996**, *37*, 9207.

Table 1. Redox Potentials of 3−6 and the Related Triarylamines[a]

compd	$E_1°'$	$E_2°'$	compd	$E_1°'$
1	+1.18[d]		**6**	+0.93[b]
3[c]	+1.12	+1.24	**9**	+1.18[d]
4[c]	+1.13	+1.57[b]	**10**	+1.32[d]
5	+0.92[b]			

[a] 0.1M n-Bu_4NClO_4 in CH_2Cl_2, potential vs SCE, Pt electrode, 25 °C, scan rate 100 mV/s. [b] Peak potential (irreversible oxidation process). [c] Measured in PhCN. [d] See ref 11.

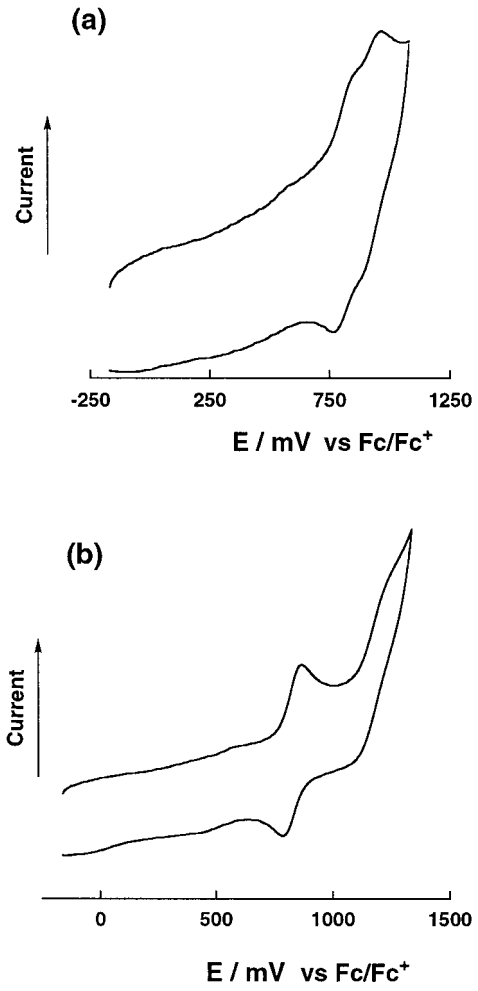

Figure 4. Cyclic voltammetry of compounds **3** and **4** in PhCN solution at room temperature with scan rate 100 mV/s.

in Figure 4, two reversible redox waves of **3** were observed in benzonitrile solution, suggesting generation of the corresponding monocation and dication. However, **4** showed only one pair of the reversible redox wave despite having the three redox-active amino groups. In cross-conjugated system like **3** and **4**, we often observe the simultaneous multielectron-transfer process. To identify whether the observed redox processes are one- or two-electron transfer, we determined the number of removed electrons by controlled-potential coulometry. As a result, the reversible redox process in **4** turned out to be two-electron-transfer process, while each redox wave in **3** turned out to be a one-electron oxidation process. From the standard potential of the related compounds, **9** and **10**,[11] it can be deduced that the two-electron oxidation

(11) Schmidt, W.; Steckhan, E. *Chem. Ber.* **1980**, *113*, 577.

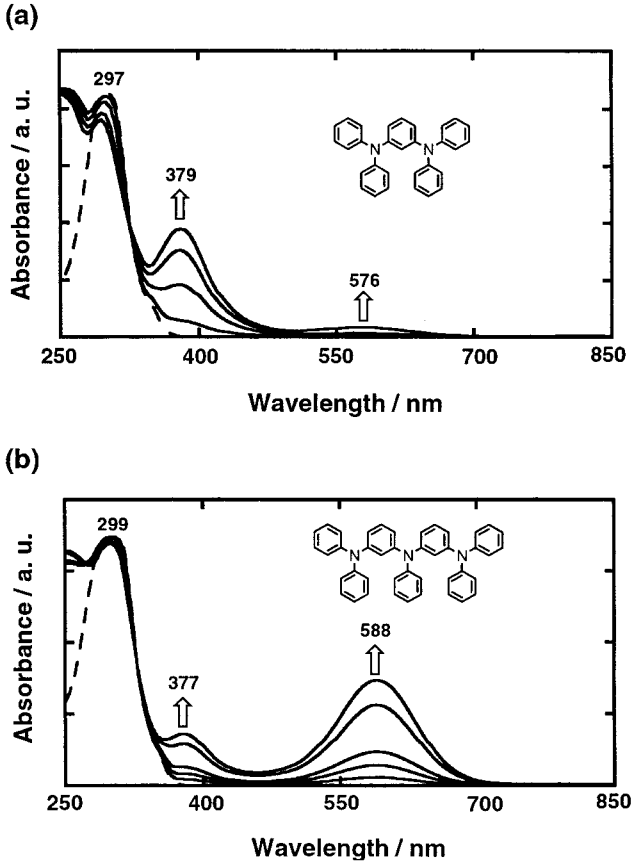

Figure 5. UV−vis spectra of the TFAA-oxidized species of (a) **5** and (b) **6** in CH_2Cl_2 at room temperature. The broken line indicates the spectrum before oxidation. The arrows designate the increase of the band at 1 h after addition of TFAA.

of **4** comes from two peripheral triarylamine units. Moreover, although assignment for the higher irreversible oxidation potential of **4** is unknown at the present stage, it probably relates to oxidation of the central triarylamine unit. Finally, it was confirmed that the second oxidation wave of **4** is irreversible even at −40 °C.

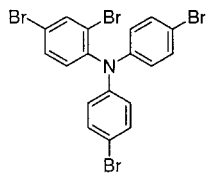

9

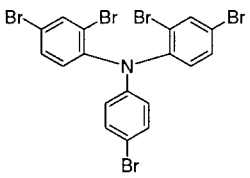

10

UV−Visible and EPR Spectra of Oxidized Species. As has been described in the preceding section, it was found that the generated cation radicals $\mathbf{5}^+$ and $\mathbf{6}^+$ are unstable and, subsequently, the follow-up reactions occur. Hence, the oxidation process of **5** and **6** was monitored by UV−vis spectroscopy. First of all, we selected trifluoroacetic anhydride, TFAA, as an oxidant. The neutral **5** (and **6**) were colorless in a CH_2Cl_2 solution that exhibits a single band at λ_{max} = 297 nm (and 299 nm). Next, the solution of **5** (and **6**) was treated with neat TFAA. After the addition of TFAA, two bands appeared gradually: **5**, λ_{max} = 379 and 569 nm; **6**, λ_{max} = 377 and 588 nm (Figure 5). The slow oxidation indicates that

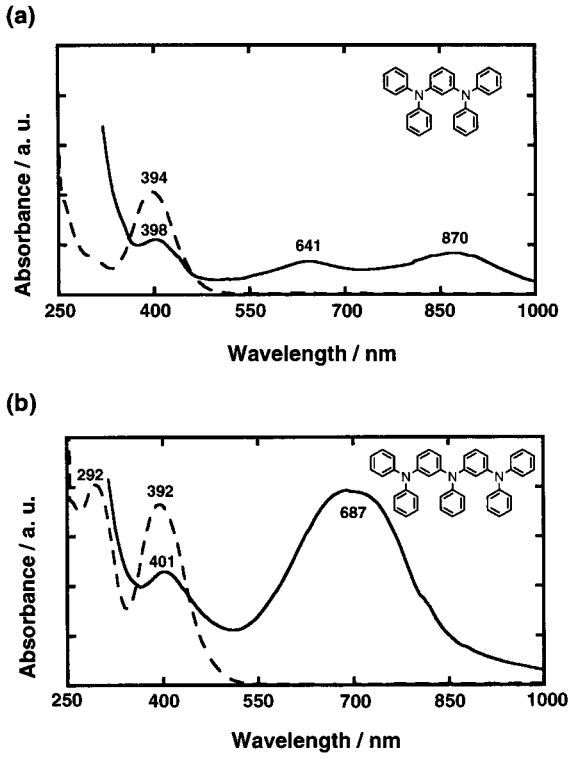

Figure 6. UV−vis spectra of the $SbCl_5$-oxidized species of (a) **5** and (b) **6** in CH_2Cl_2 at room temperature. The broken line indicates the spectrum before oxidation.

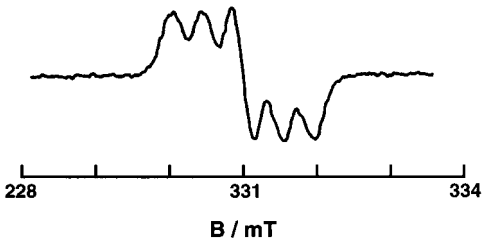

Figure 7. EPR spectrum of the TFAA-oxidized species of **6** in CH_2Cl_2 at room temperature.

TFAA is a weak oxidant for **5** and **6**. In contrast with TFAA, when $SbCl_5$ was used for oxidation of **5** and **6** in a CH_2Cl_2/trifluoroacetic acid (TFA) (=3/1 (v/v)) mixture, the oxidation process was accomplished immediately and, moreover, the absorption spectra of the $SbCl_5$-oxidized species differed much from those of the TFAA-oxidized ones (Figure 6). Note that the spectra of **5** (and **6**) before oxidation showed a single additional band at 394 nm (and 392 nm) probably owing to TFA. Upon addition of a few drops of neat $SbCl_5$, the band at about 390 nm decreased, and new and broad bands appeared in the lower energy region: **5**, λ_{max} = 641 and 870 nm; **6**, λ_{max} = 687 nm. These findings clearly indicate the formation of highly π-conjugated compounds by the follow-up reactions. The corroborating evidence was obtained from the EPR spectrum of the oxidized solution (Figure 7). The observed quintet spectrum was typical for benzidine cation radical with an unpaired electron equally coupled to two nitrogen atoms (a_N = 0.43 mT).[12] This suggests that the further

(12) (a) Dollish, F. R.; Hall, W. K. *J. Phys. Chem.* **1965**, *69*, 2127. (b) Seo, E. T.; Nelson, R. F.; Fritsch, J. M.; Marcoux, L. S.; Leedy, D. W.; Adams, R. N. *J. Am. Chem. Soc.* **1966**, *88*, 3498.

Scheme 2. Schematic Oxidation Pathway of 4

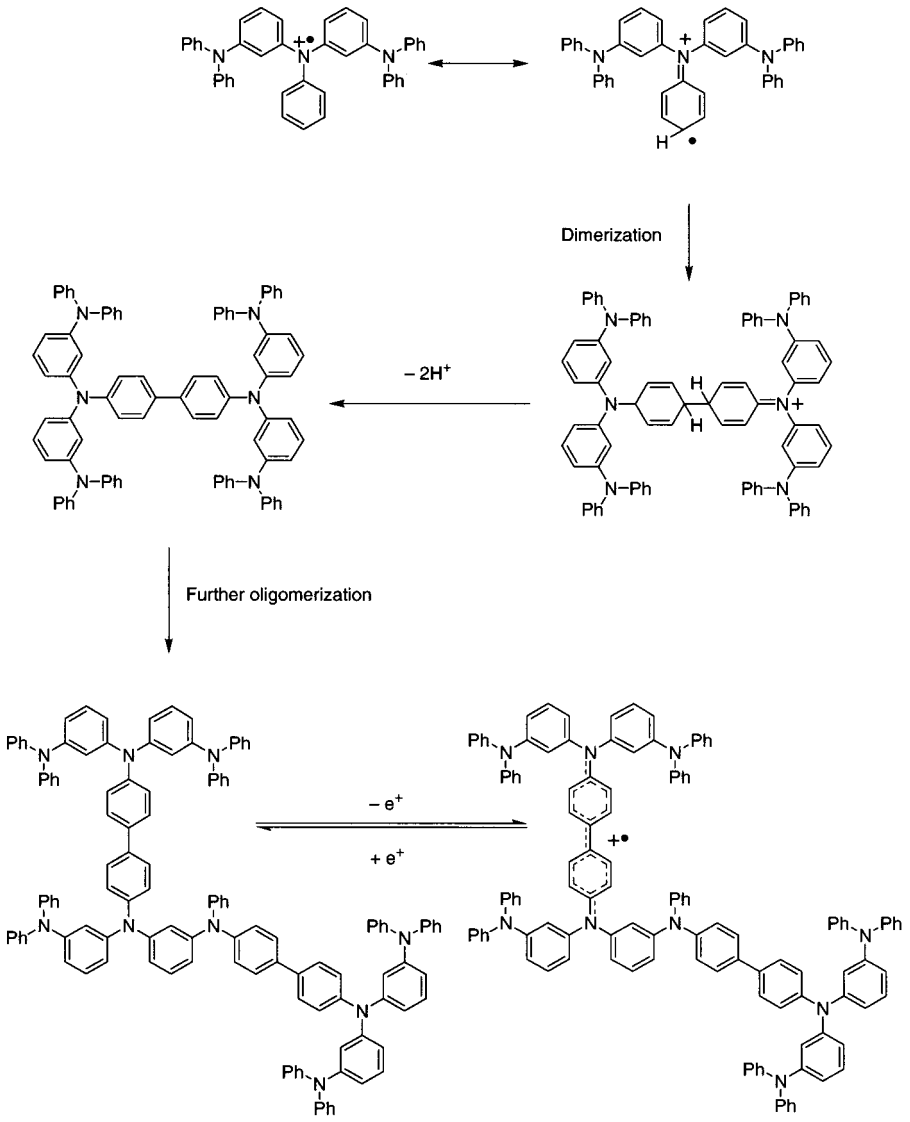

oligomerization reactions between the generated cation radicals $\mathbf{5}^+$ (and $\mathbf{6}^+$) took place because of their high spin density at the *ortho*- and *para*-ring positions.[13] Of the resulting products, those containing benzidine moieties are more easily oxidized than the parent **5** (and **6**) and, finally, undergo further oxidation to the benzidine cation radical exhibiting the above-mentioned characteristic EPR spectrum (Scheme 2). The appearance of the different absorption spectra due to the different oxidants is probably ascribed to the resulting oligomerized products.

Contrary to **5** and **6**, the above oligomerization reaction is difficult for all-*para*-brominated oligomers **3** and **4**. Judging from the oxidation potentials of **3** and **4**, $SbCl_5$ is pertinent to oxidize these compounds. Addition of less than 1 equiv of $SbCl_5$ into a CH_2Cl_2 solution of **3** (and **4**) yielded a blue solution showing a single EPR signal without any hyperfine structures [$\Delta B_{pp} = 1.52$ mT for $\mathbf{3}^+$ ($\Delta B_{pp} = 1.57$ mT for $\mathbf{4}^+$)]. As shown in Figure 8, the resulting solution for $\mathbf{3}^+$ (and $\mathbf{4}^+$) showed a single broad band at 779 nm (790 nm), which is clearly different from the spectra for the oxidized products of **5** (and **6**). This suggests that the cation radical of the all-*para*-brominated **3** (and **4**) was highly stable at room temperature in accordance with the results of the CV studies. Actually, both $\mathbf{3}^+$ and $\mathbf{4}^+$ were isolated from the CH_2Cl_2 solution by adding diethyl ether. However, we have not hitherto succeeded in obtaining single crystals suitable for the X-ray diffraction study.

As a result of the CV measurements, **3** and **4** are expected to generate the di- or trication by excess of $SbCl_5$. The resulting EPR spectra in frozen CH_2Cl_2 solution of **3** (and **4**) showed a similar single signal with broad line width compared with $\mathbf{3}^+$ (and $\mathbf{4}^+$) [$\Delta B_{pp} = 1.95$ mT for **3** ($\Delta B_{pp} = 2.80$ mT for **4**)] (Figure 9). More noteworthy is that, in both samples, a weak transition was observed in the $\Delta m_S = \pm 2$ region, clearly indicating the presence of high-spin species. To identify the spin multiplicity of this species, we adopted the pulsed EPR method on the basis of the the fact that the magnetic moments with distinct spin quantum numbers (S) precess with their specific nutation frequency (ω_n) in the presence of a microwave irradiation field (B_1) and a static magnetic field (B_0).[14] If the microwave irradiation field ($\omega_1 = -\gamma_e B_1$) is weak enough compared with the fine-structure parameter (ω_D in units of frequency), the nutation frequency

(13) (a) Ito, A.; Miyajima, H.; Yoshizawa, K.; Tanaka, K.; Yamabe, T. *J. Org. Chem.* **1997**, *62*, 38. (b) Ito, A.; Ono, Y.; Tanaka, K. *J. Org. Chem.* **1999**, *64*, 8236.

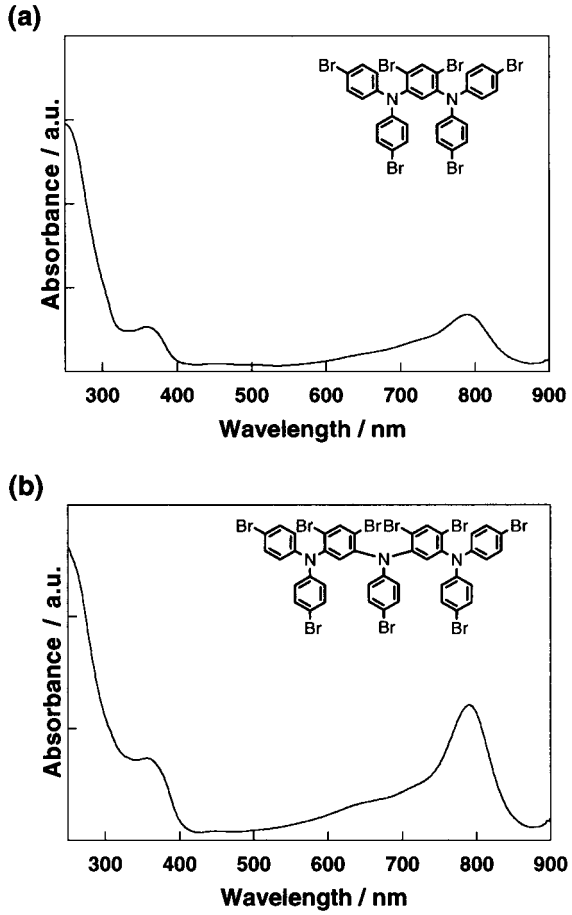

Figure 8. UV−vis spectra of (a) **3** and (b) **4** oxidized by less than 1 equiv of $SbCl_5$ in CH_2Cl_2 at room temperature.

for a transition from $|S, M_S\rangle$ to $|S, M_S+1\rangle$ is expressed in good approximation as

$$\omega_n = [S(S+1) - M_S(M_S+1)]^{1/2}\omega_1 \qquad (1)$$

indicating that ω_n can be scaled with the spin quantum numbers S and M_S in a unit of ω_n ($=\omega_1$) for the doublet species. Figure 10 shows the relation between the EPR spectra observed at 5 K and its transient nutation spectra in a 2-D contour representation. Namely, the projection on the magnetic field axis roughly corresponds to the usual EPR spectrum, while the projection on the frequency axis corresponds to the nutation spectrum. The intense peak observed at 341.0 mT (341.5 mT) is expected to be the $|1/2, +1/2\rangle \leftrightarrow |1/2, -1/2\rangle$ transition of the doublet species $\mathbf{3}^+$ ($\mathbf{4}^+$) and had the nutation frequency of 30.0 MHz (30.0 MHz), indicating $\omega_1 = 30$ MHz. On the other hand, two peaks at 332.5 and 351.0 mT (339.5 and 344.5 mT) had the same nutation frequency of 43.8 MHz (43.9 MHz), suggesting the presence of a high-spin cationic species of **3** (**4**). Here, the frequency ratio (ω_n/ω_1) of 43.8/30.0 (43.9/30.0) is in good agreement with the ratio of $\sqrt{2}$ expected for $|1, 0\rangle \leftrightarrow |1, \pm1\rangle$ transition of the triplet

(14) For determination of spin-multiplicity for high-spin molecules by using pulsed EPR technique, see: (a) Isoya, J.; Kanda, H.; Norris, J. R.; Tang, J.; Bowman, M. K. *Phys. Rev.* **1990**, *B41*, 3905. (b) Astashkin, A. V.; Schweiger, A. *Chem. Phys. Lett.* **1990**, *174*, 595. (c) Sato, K.; Yano, M.; Furuichi, M.; Shiomi, D.; Takui, T.; Abe, K.; Itoh, K.; Higuchi, A.; Katsuma, K.; Shirota, Y. *J. Am. Chem. Soc.* **1997**, *119*, 6607. (d) Bock, H.; Gharagozloo-Hubmann, K.; Sievert, M.; Prisner, T.; Havlas, Z. *Nature* **2000**, *404*, 267.

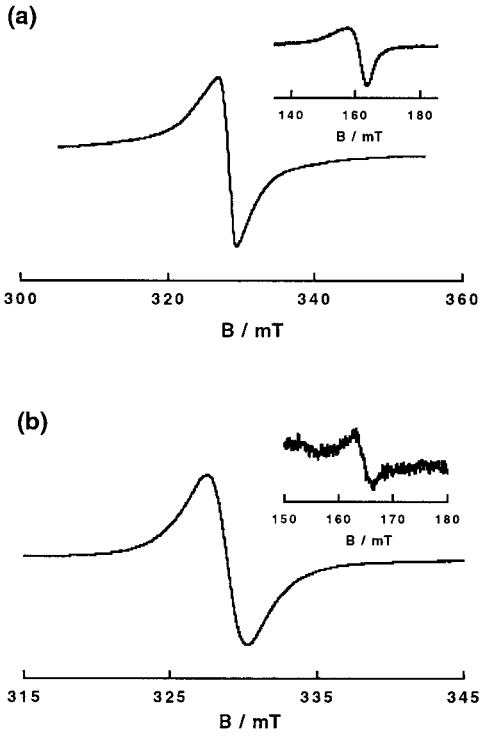

Figure 9. EPR spectra of (a) **3** and (b) **4** oxidized by excess $SbCl_5$ in CH_2Cl_2 at 123 K. Inset: Spectra for the forbidden $\Delta m_S = \pm 2$ transition at 123 K.

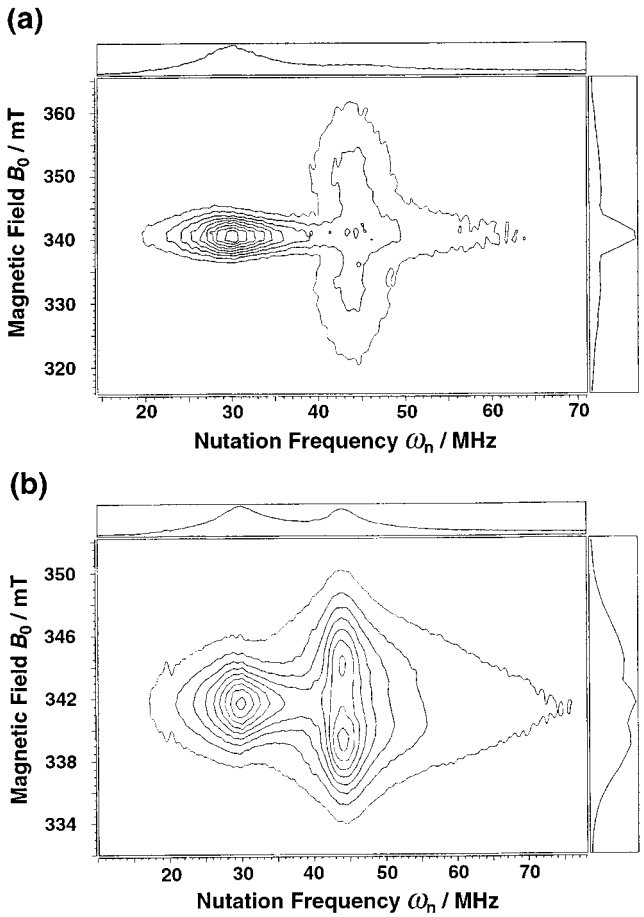

Figure 10. Field-swept electron spin nutation spectra of (a) **3** and (b) **4** oxidized by excess $SbCl_5$ in CH_2Cl_2 at 5 K. ω_1 corresponds to 30 MHz.

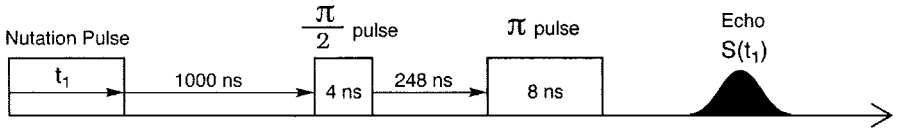

Figure 11. Pulse sequence for the measurements of the electron spin nutation spectrum.

Table 2. Summary of Crystal Data, Data Collection, and Refinement Parameters for 3−5

	3	**4**	**5**
formula	$C_{31}H_{20}Br_6N_2Cl_2$	$C_{42}H_{24}Br_9N_3$	$C_{60}H_{48}N_4$
M_r	970.84	1289.81	825.07
cryst habit	colorless plate	colorless plate	colorless prismatic
cryst size (mm)	0.91 × 0.24 × 0.06	0.63 × 0.15 × 0.06	0.50 × 0.45 × 0.30
cryst system	monoclinic	triclinic	monoclinic
space group	$P2_1/n$	$P\bar{1}$	Cc
cell consts			
a (Å)	16.003(4)	10.558(2)	25.192(2)
b (Å)	11.986(5)	20.992(3)	9.811(2)
c (Å)	18.377(4)	10.298(2)	19.412(5)
α (deg)	92.79(1)		
β (deg)	109.68(2)	106.41(2)	104.48(1)
γ (deg)	100.85(2)		
V (Å^3)	3319(1)	2137.7(7)	4645(1)
Z	4	2	8
D_{calcd} (g cm^{-3})	1.943	2.004	2.359
μ (mm^{-1})	74.65	84.98	1.37
F(000)	1856.00	1224.00	3488.00
$2\theta_{max}$	55.0	50.0	55.0
no. of reflcns			
measd	8272	6392	4467
unique	7994	5947	4345
R_{int}	0.072	0.053	0.031
Params	390	511	578
R (R_w)	0.063 (0.069) [$I > 3.00\sigma(I)$]	0.075 (0.082) [$I > 3.00\sigma(I)$]	0.056 (0.031) [$I > 2.00\sigma(I)$]
max $\Delta\rho$ (e Å^{-3})	1.10	0.95	0.15

state from eq 1. As a result, the high-spin species generated by excess of $SbCl_5$ can be regarded as $\mathbf{3}^{2+}$ ($\mathbf{4}^{2+}$). Therefore, it was found that the broad EPR spectra shown in Figure 9 should be viewed as overlap of the doublet and triplet spectra. The reason the quartet state expected for $\mathbf{4}^{3+}$ was not observed is probably due to weakness of the oxidant employed. It is noteworthy that the D values of $\mathbf{3}^{2+}$ and $\mathbf{4}^{2+}$, which cannot be determined from the usual EPR measurements (Figure 9), can be approximately estimated to be 9.25 and 2.25 mT from the peak-to-peak width at ω_n = ca. 44 MHz. From these values, the average distances between two radical centers of $\mathbf{3}^{2+}$ and $\mathbf{4}^{2+}$ are roughly calculated to be 6.7 and 10 Å, respectively, by using the so-called point dipole approximation. The estimated distance of 6.7 Å is a little longer than the distance between two nitrogen atoms in **3**. On the other hand, 10 Å is in good agreement with the distance between the two peripheral nitrogen atoms if $\mathbf{4}^{2+}$ adopts an expanded conformation in contrast to the U-shape conformation of the X-ray structure. This suggests that the positive charge in $\mathbf{4}^{2+}$ is localized on the two peripheral triphenylamino moieties and, moreover, $\mathbf{4}^{2+}$ adopts a linear conformation so as to diminish the intramolecular Coulomb repulsion.

Conclusions

We have shown that the use of $(BTMA)Br_3$ leads selectively and completely to Br substitution at all the *para* positions of oligo(*N*-phenyl-*m*-aniline)s. The U-shaped structure of **4** suggests that the polymerization process to poly(*N*-aryl-*m*-aniline)s entails the formation of cyclic oligomers and, moreover, the resulting polymer readily adopts helical structures. The oxidized species of the Br-unsubstituted **5** and **6** caused complicated follow-up reactions toward a mixture of the higher oligomeric products containing benzidine cation radical moieties. On the other hand, the Br-substituted **3** and **4** gave thermally stable and isolable cation radicals. Furthermore, it was confirmed that the oxidation of **3** and **4** in CH_2Cl_2 with an excess of $SbCl_5$ generates the high-spin bis-cation radicals $\mathbf{3}^{2+}$ and $\mathbf{4}^{2+}$. The reason for difficulty of additional electron removal from $\mathbf{4}^{2+}$ resides probably on the increase of oxidation potentials due to polybromo substitutions.

Experimental Section

General Procedures. Commercial grade reagents were used without further purification. Elemental analyses were performed by Microanalytical Center, Kyoto University.

Physical Measurements. The CV measurements were performed with a combination of Hokuto-Denko HA-305 potentiostat, HB-104 function generator, and Yokogawa 3025 XY recorder with a three-electrode cell using Pt wires as the working and the counter electrodes and an Ag/0.01 M $AgNO_3$ (MeCN) as the reference electrode in a solution of 0.25 mM of **5** (or **6**) and 0.1 M n-Bu_4NClO_4 in CH_2Cl_2 (25 °C, scan rate 100 mV s^{-1}). On the other hand, a BAS CV-50W voltammetric analyzer was employed for the CV and coulometry measurements of **3** and **4** in PhCN (0.4 mM). The observed potentials were corrected with reference to ferrocene added as an internal standard after each measurement. UV−vis spectra were recorded on a Shimadzu UV-2200 spectrometer. EPR spectra were measured using a JEOL JES-RE-2X X-band spectrometer. Pulsed EPR measurements were carried out on a Bruker ELEXES E580 X-band FT ESR spectrometer. The microwave pulse sequence used is shown in Figure 11. For the transient nutation experiment, the two-pulse electron spin−echo signal $S(t_1)$ was detected by increasing the width (t_1) of the nutation

pulse. We employed phase cycles to suppress unwanted signals and artifacts which arise from an inaccurate pulse length. The observed signal $S(t_1, B_0)$ as a function of the external magnetic field B_0 is converted into a nutation frequency domain $S(\omega_N, B_0)$ spectrum by Fourier transformation along the t_1 direction, as shown in Figure 10.

***N,N,N′,N′*-Tetraphenyl-1,3-benzenediamine (5).** Diphenylamine (8.60 g, 50.8 mmol), 1,3-dibromobenzene (6.00 g, 25.4 mmol), CuI (0.48 g, 2.5 mmol), 18-crown-6 (0.66 g, 2.5 mmol), and K_2CO_3 (7.00 g, 50.6 mmol) were heated together at 200 °C for 24 h with stirring under N_2 atmosphere. The reaction mixture was poured into ethyl acetate, and the inorganic impurity was removed by filtration. After evacuation of ethyl acetate, the remaining mixture was column-chromatographed on silica gel (eluent: *n*-hexane) to afford **5** (R_f = 0.37) as a white solid in 27% yield. Mp: 140−141 °C. ^{1}H NMR ($CDCl_3$, 300 MHz) [δ (ppm)]: 6.65 (dd, 2H), 6.87 (t, 1H); 6.95 (tt, 4H); 7.05 (m, 9H); 7.20 (m, 8H). ^{13}C NMR ($CDCl_3$, 75 MHz) [δ (ppm)]: 118.3, 119.7, 122.6, 124.0, 129.1, 129.7, 147.5, 148.5. Anal. Calcd for $C_{30}H_{24}N_2$: C, 87.35; H, 5.86; N, 6.79. Found: C, 87.27; H, 5.65; N, 6.76.

3,3′-Dinitrotriphenylamine (7). 3-Iodonitrobenzene (6.22 g, 25.0 mmol), aniline (1.00 g, 10.7 mmol), CuI (0.48 g, 2.5 mmol), 18-crown-6 (0.53 g, 2.0 mmol), K_2CO_3 (3.45 g, 25.0 mmol), and *o*-dichlorobenzene (5 mL) were heated together at 180 °C for 24 h with stirring under N_2 atmosphere. The reaction mixture was poured into ethyl acetate, and the inorganic impurity was removed by filtration. After evacuation of ethyl acetate, the remaining mixture was column-chromatographed on silica gel (eluent: 1:4 ethyl acetate−*n*-hexane) to afford **7** (R_f = 0.53) as a brown solid in 45% yield. ^{1}H NMR ($CDCl_3$, 90 MHz) [δ (ppm)]: 7.08−7.40 (m, 9H), 7.88 (m, 4H). Anal. Calcd for $C_{18}H_{13}N_3O_4$: C, 64.47; H, 3.91; N, 12.53. Found: C, 64.60; H, 3.79; N, 12.56.

3,3′-Diaminotriphenylamine (8). **7** (1.47 g, mmol) dissolved in MeCN (35 mL) at 50 °C was added quickly into a hot solution (ca. 50 °C) of $SnCl_2$ in concentrated HCl (24 mL) with stirring. After being stirred for 1 h at ca. 60 °C, the resulting mixture was made alkaline enough so as not to deposit inorganic white colloids and extracted with Et_2O. The Et_2O solution was dried over $MgSO_4$. After column chromatography on silica gel (eluent: 1:1 ethyl acetate−*n*-hexane), **8** (R_f = 0.51) was obtained as a white solid (yield 89%). ^{1}H NMR ($CDCl_3$, 90 MHz) [δ (ppm)]: 3.90 (br s, 4H), 5.93−7.27 (m, 13H). Anal. Calcd for $C_{18}H_{17}N_3$: C, 78.52; H, 6.22; N, 15.26. Found: C, 78.03; H, 6.58; N, 15.12.

3,3′-Bis(diphenylamino)triphenylamine (6). **8** (0.73 g, 2.7 mmol), iodobenzene (10.8 g, 53.0 mmol), CuI (1.00 g, 5.2 mmol), and K_2CO_3 (1.50 g, 10.9 mmol) were heated together at 180 °C for 64 h with stirring under N_2 atmosphere. The reaction mixture was poured into ethyl acetate, and the inorganic impurity was removed by filtration. After evacuation of ethyl acetate, the remaining mixture was column-chromatographed on silica gel (eluent: 1:9 ethyl acetate−*n*-hexane) to afford **6** (R_f = 0.77) as a pale yellow solid in 38% yield. Mp: 121−122 °C. ^{1}H NMR ($CDCl_3$, 270 MHz) [δ (ppm)]: 6.66 (m, 4H), 6.84−7.22 (m, 29H). ^{13}C NMR ($CDCl_3$, 67.5 MHz) [δ (ppm)]: 118.5, 118.6, 119.9, 122.4, 122.7, 123.5, 124.1, 129.0, 129.1, 129.7, 147.3, 147.5, 148.3, 148.6. Anal. Calcd for $C_{42}H_{33}N_3$: C, 87.01; H, 5.74; N, 7.25. Found: C, 86.50; H, 5.99; N, 7.08.

4,6-Dibromo-1,3-bis[bis(4-bromophenyl)amino]benzene (3). To a mixed solution (CH_2Cl_2 5 mL, MeOH 2 mL) of **5** (0.30 g, 0.73 mmol) was added K_2CO_3 (0.60 g, 4.4 mmol) and then a mixed solution (CH_2Cl_2, 5 mL; MeOH, 2 mL) of benzyltrimethylammonium tribromide (1.70 g, 4.36 mmol) dropwise with stirring. After being stirred for 1 h until the orange color faded away, the reaction mixture was allowed to stand for 1 day. The precipitated white crystals were filtered out, and the inorganic impurity was washed out with a quantity of water. The resulting crystals were, furthermore, washed with a portion of $CHCl_3$. Colorless plates (0.47 g, 67%) were obtained. Mp: 271−272 °C. ^{1}H NMR ($CDCl_3$, 270 MHz) [δ (ppm)]: 5.30 (s, 1H), 6.78 (d, J = 8.8 Hz, 8H); 7.33 (d, J = 8.8 Hz, 8H); 7.89 (s, 1H). ^{13}C NMR ($CDCl_3$, 67.5 MHz) [δ (ppm)]: 115.7, 120.7, 119.9, 123.6, 132.4, 132.7, 139.7, 145.0, 145.5. Anal. Calcd for $C_{30}H_{18}N_2Br_6 \cdot C_1H_2Cl_2$: C, 38.35; H, 2.08; N, 2.89. Found: C, 38.14; H, 2.11; N, 2.85.

4,4′,4″,6,6′-Pentabromo-3,3′-bis[bis(4-bromophenyl)amino]triphenylamine (4). To a mixed solution (CH_2Cl_2, 5 mL; MeOH, 2 mL) of **6** (0.26 g, 0.45 mmol) was added K_2CO_3 (0.55 g, 4.0 mmol) and then a mixed solution (CH_2Cl_2, 5 mL; MeOH, 2 mL) of benzyltrimethylammonium tribromide (1.58 g, 4.05 mmol) dropwise with stirring. After being stirred for 1 h until the orange color faded away, the reaction mixture was allowed to stand for 1 day. After evaporation of the solvent, the residue was separated into the aqueous and CH_2Cl_2 layers. The CH_2Cl_2 solution was dried over $MgSO_4$. After evaporation of the solvent, the resulting yellow solids were recrystallized from CH_2Cl_2−MeOH (5:2). Yellow plates (0.37 g, 64%) were obtained. Mp: 257−258 °C. ^{1}H NMR ($CDCl_3$, 270 MHz) [δ (ppm)]: 6.60 (d, J = 8.6 Hz, 2H), 6.64 (s, 2H), 6.71 (d, J = 8.9 Hz, 8H), 7.27 (d, J = 8.6 Hz, 2H), 7.30 (d, J = 8.9 Hz, 8H); 7.80 (s, 2H). ^{13}C NMR ($CDCl_3$, 67.5 MHz) [δ (ppm)]: 115.7, 116.1, 118.3, 118.8, 123.2, 123.7, 129.7, 132.3, 139.6, 140.5, 144.5, 144.9, 145.0, 145.2. Anal. Calcd for $C_{42}H_{24}N_3Br_9$: C, 39.11; H, 1.88; N, 3.26; Br, 55.76. Found: C, 38.78; H, 1.72; N, 3.09; Br, 58.09.

X-ray Structural Analysis of 3−5. Single-crystal diffraction experiments were carried out at room temperature on a Rigaku AFC7R four-circle diffractometer equipped with graphite-monochromated Mo Kα radiation using the $\omega\angle 2\theta$ scan technique. The data were corrected for Lorentz and polarization effects. In addition, a ψ-scan empirical absorption was applied for **3** and **4** (several reflections; minimum, maximum transmission 0.23, 1.00 for **3** and 0.47, 1.00 for **4**). The structures were solved by direct methods using SHELXS 86[15] (for **3** and **4**) and SAPI 91[16] (for **5**), expanded using DIRDIF92.[17] The non-hydrogen atoms were refined by full-matrix least-squares analysis with the anisotropic thermal parameters. After several cycles of refinements, the position of the H atoms were calculated and fixed. All the calculations were performed using teXsan crystallographic software package of Molecular Structure Corp.[18] Crystal data and experimental details are listed in Table 2. Full structural information has been deposited with the Cambridge Crystallographic Data Centre.[19]

Acknowledgment. This work was supported by a Grant-in-Aid for Scientific Research from the Ministry of Education, Science, and Culture of Japan.

JO0160571

(15) Sheldrick, G. M. SHELXS 86, Program for the Solution of Crystal Structures, University of Göttingen, 1986; *Acta Crystallogr., Sect. A* **1990**, *46*, 467.

(16) Hai-Fu, F. *SAPI91, Structure Analysis Programs with Intelligent Control*; Rigaku Corp.: Tokyo, Japan, 1991.

(17) Beurskens, P. T.; Admiraal, G.; Beurskens, G.; Bosman, W. P.; Garcia-Granda, S.; Gould, R. O.; Smits J. M. M.; Smykalla, C. *DIRDIF program system*; Technical Report of the Crystallography Laboratory, University of Nijmegen: Nijmegen, The Netherlands, 1992.

(18) *TEXSAN 1.8, Crystal Structure Analysis Package*; Molecular Structure Corp.: The Woodlands, TX, 1997.

(19) Supplementary publication nos. CCDC-167826 (**3**), -167825 (**4**), and -167824 (**5**) can be obtained on request from the Director, Cambridge Crystallographic Data Centre, 12 Union Road, Cambridge CB12 1E2, U.K.